



## Sudden disappearance of yew (*Taxus baccata*) woodlands from eastern England coincides with a possible climate event around 4.2 ka ago

Tatiana Bebchuk<sup>a,\*</sup>, Paul J. Krusic<sup>a</sup>, Joshua H. Pike<sup>a</sup>, Alma Piermattei<sup>b,c</sup>, Ronny Friedrich<sup>d</sup>, Lukas Wacker<sup>e</sup>, Alan Crivellaro<sup>c</sup>, Tito Arosio<sup>a</sup>, Alexander V. Kirilyanov<sup>a</sup>, Philip Gibbard<sup>f</sup>, David Brown<sup>g</sup>, Jan Esper<sup>h,i</sup>, Frederick Reinig<sup>h</sup>, Ulf Büntgen<sup>a,i,j,k</sup>

<sup>a</sup> Department of Geography, University of Cambridge, CB2 3EN, Cambridge, United Kingdom

<sup>b</sup> Department of Agricultural, Forest and Food Sciences, University of Torino, Largo Paolo Braccini, 2, 10095, Grugliasco, TO, Italy

<sup>c</sup> Forest Biometrics Laboratory, Faculty of Forestry, Stefan cel Mare University of Suceava, 720229, Suceava, Romania

<sup>d</sup> Curt-Engelhorn-Centre Archaeometry, 68159, Mannheim, Germany

<sup>e</sup> Laboratory of Ion Beam Physics, ETHZ, Otto-Stern Weg 5 HPK, 8093, Zurich, Switzerland

<sup>f</sup> Scott Polar Research Institute, University of Cambridge, CB2 1ER, Cambridge, United Kingdom

<sup>g</sup> School of Natural and Built Environment, The Queen's University, Belfast, BT7 1NN, United Kingdom

<sup>h</sup> Department of Geography, Johannes Gutenberg University, 55099, Mainz, Germany

<sup>i</sup> Global Change Research Institute (CzechGlobe), Czech Academy of Sciences, 60300, Brno, Czech Republic

<sup>j</sup> Swiss Federal Research Institute (WSL), 8903 Birmensdorf, Switzerland

<sup>k</sup> Department of Geography, Faculty of Science, Masaryk University, 611 37, Brno, Czech Republic

### ARTICLE INFO

Handling Editor: Donatella Magri

#### Keywords:

Dendrochronology  
Forest dynamics  
Mid-Holocene  
Palaeoecology  
Radiocarbon dating  
Sea-level changes  
Subfossil wood  
Tree rings

### ABSTRACT

Tree-ring chronologies form the backbone of high-resolution palaeoclimatology. However, their number declines drastically prior to medieval times, and only a few such records worldwide extend back to the mid-Holocene. Here, we present a collection of more than 400 subfossil yew (*Taxus baccata* L.) trees excavated from near sea-level peat-rich sediments in the Fenland region of eastern England. The well-preserved yew trunks are between two and eight metres long, often exhibit adventitious root layers, and contain up to 400 rings of highly irregular growth. Combined dendrochronological and radiocarbon dating resulted in two tree-ring width chronologies that comprise 36 and 32 trees, span 413 and 418 years, exhibit mean inter-series correlations ( $R_{bar}$ ) of 0.50 and 0.51, and were provisionally dated to 5225–4813 ( $\pm 4$ ) and 4612–4195 ( $\pm 6$ ) years cal BP. Together with a total of 63 radiocarbon dates ( $^{14}C$ ), our subfossil tree-ring evidence suggests that yew establishment (or onset of preservation) began  $\sim 5250$  years cal BP and resulted in extensive climax forests between 5200 and 4200 years cal BP. A first stage of yew decline  $\sim 4800$ –4600 years cal BP was possibly caused by oxygen deprivation from soil wetting, whereas yew disappearance  $\sim 4200$  years cal BP is suggested to have been triggered by marine inundation as a consequence of rapid sea-level rise. Both phases of yew decline in eastern England coincide with marked reductions in subfossil oak and pine from peatbogs in Ireland, Germany and the Netherlands. Our results emphasise the potential to develop a dendrochronological network in coastal England for better understanding of larger-scale climate and environmental changes during the mid-Holocene, including the still debated 4.2 ka climate event. Moreover, we expect our subfossil yew chronologies to facilitate the dating of local archaeological remains, refine sea-level reconstructions around the British Isles, and contribute to the international radiocarbon calibration curve IntCal.

### 1. Introduction

Tree-ring width (TRW) chronologies have provided annually resolved and absolutely dated information on temperature or

hydroclimate variability over past centuries to millennia (Fritts, 1976). Although dendroclimatic evidence forms the backbone of high-resolution palaeoclimatology (Esper et al., 2016; Ljungqvist et al., 2020), the number of TRW chronologies that extend beyond medieval

\* Corresponding author.

E-mail address: [tb649@cam.ac.uk](mailto:tb649@cam.ac.uk) (T. Bebchuk).

<https://doi.org/10.1016/j.quascirev.2023.108414>

Received 31 August 2023; Received in revised form 2 November 2023; Accepted 3 November 2023

Available online 24 November 2023

0277-3791/© 2023 The Authors. Published by Elsevier Ltd. This is an open access article under the CC BY license (<http://creativecommons.org/licenses/by/4.0/>).

times declines drastically (Biondi et al., 2023; Büntgen et al., 2022). Owing to a general decrease in the quality and quantity of relict (subfossil) wood back in time (Tegel et al., 2022), there are currently only 17 published TRW chronologies worldwide that continuously cover the past 4000 years and were used for palaeoenvironmental interpretations (Table S1). From these 17 chronologies, 11 are based on dry-dead wood remains from mountainous environments: a 4154-year-long Huon pine chronology from Tasmania (Allen et al., 2014; Cook et al., 2000), a 5681-year-long Patagonian cypress chronology from Chile (Lara et al., 2020), two Qilian juniper chronologies of 4648 and 6691 years from the Tibetan Plateau (Yang et al., 2014, 2021), and seven bristlecone pine chronologies from Nevada and California, which vary between 4350 and 8683 years in length (Ferguson, 1969; Ferguson et al., 2002; Ferguson and Graybill, 1983; Graybill, 1996, 2002; Salzer, 2010; Salzer and Hughes, 2010a, 2010b). Over western Europe, TRW measurements of

subfossil wood from peatbogs in Northern Ireland and England have produced a 7272-year-long Belfast oak chronology (Pilcher et al., 1984), and waterlogged Scots pine wood from lacustrine deposits have been used to develop two 7417 and 7639-year-long chronologies from Sweden (Grudd et al., 2002) and Finland (Helama et al., 2008), respectively. Alluvial deposits of large river systems provided sufficient wood for an 8768-year-long Siberian larch chronology from the Yamal Peninsula (Hantemirov et al., 2021), and a 10,085-year-long chronology was developed from subfossil stone pine, larch and spruce wood from high-elevation glacier forefields, lacustrine deposits, and peatbogs in the eastern Alps (Nicolussi et al., 2015). The world's longest TRW chronology spans the past 12,460 years and was built from subfossil oak and pine wood collected in fluvial deposits across Germany (Friedrich et al., 2004). Further to these continuous TRW chronologies, subfossil wood remains from extensive peatlands in Sweden (Edvardsson et al., 2012a),

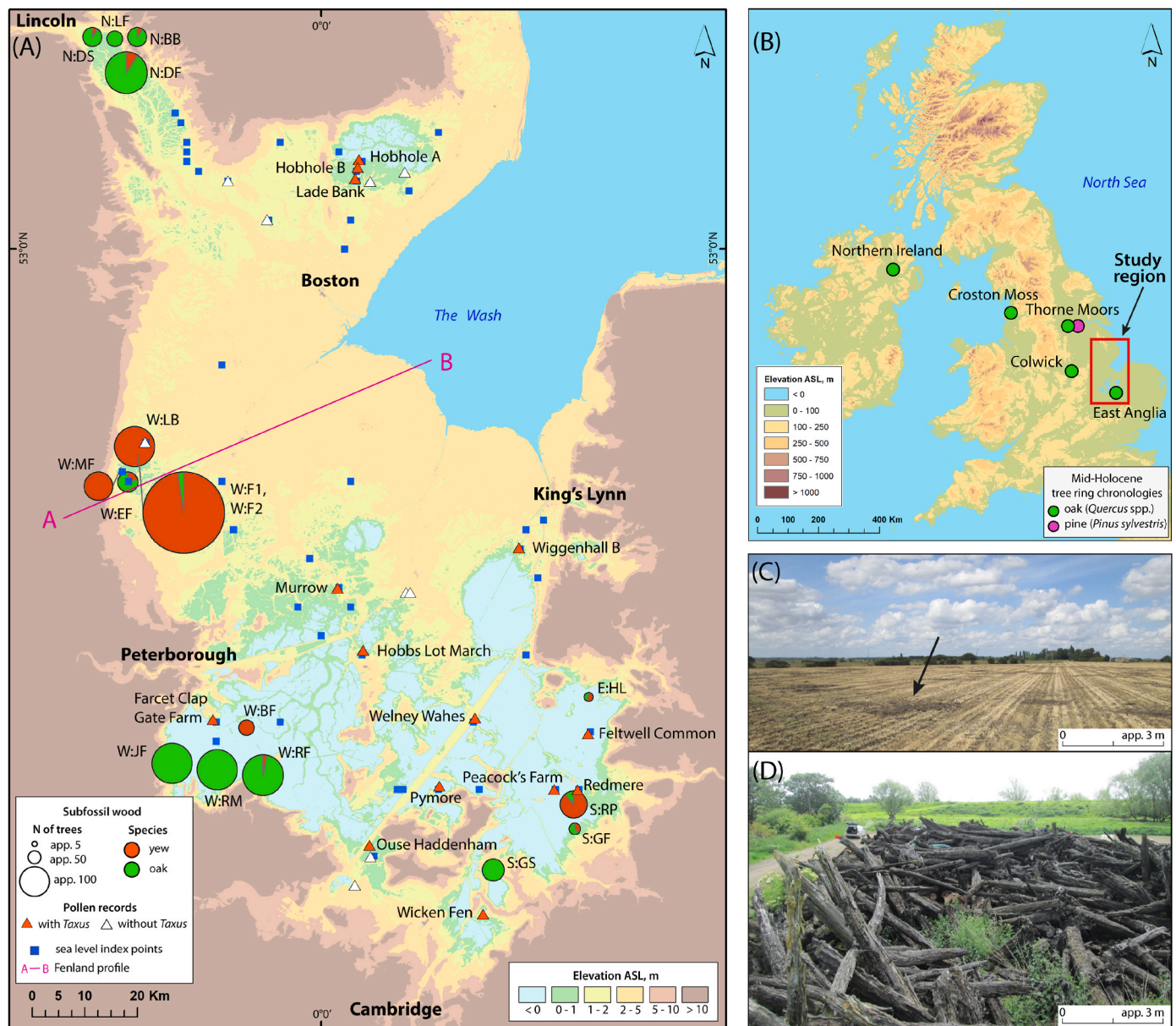


**Fig. 1.** (A) Topographical map of the Fenland with piles of subfossil wood visited in 2020–2023. Circle sizes correspond with pile size, and colours indicate tree species. Pollen records shown as triangles (white if no *Taxus* pollen were identified, and orange otherwise), and marine index points used for sea-level reconstructions shown as blue squares, after Waller (1994). The A-B line indicates the position of the profile shown in Fig.6. (B) Topographical map of the United Kingdom with the approximate locations of mid-Holocene TRW chronologies (Baillie and Brown, 1988; Boswijk and Whitehouse, 2002). (C) Agricultural field in the Fenland. Note the dark holes, from which subfossil trunks were excavated in August 2022. (D) Pile of subfossil yew trunks at site W:F1, at north of Peterborough. Colours must be used in print.

Denmark (Christensen, 2007), Germany (Eckstein et al., 2009), Scotland (Moir, 2012), and England (Baillie and Brown, 1988) were essential for the development of TRW chronologies covering the fifth and fourth millennia before present (cf. Tegel et al., 2022 for a review on European dendroarchaeology and Edvardsson et al., 2016 for a review on peatbog dendrochronology).

The Fenland in eastern England is a peat-rich coastal lowland region that is circa -3 to 2 m above sea-level (m a.s.l.). This basin was formed during the Late Wolstonian glaciation ~180–150 kyr BP (Gibbard et al., 2021) and extends from Cambridge in the south to Lincoln in the north, and from Peterborough in the west to King's Lynn in the east (Fig. 1). During the Last Glacial Maximum (LGM; ~23–19 kyr BP; Hughes and Gibbard, 2015) the ice-free Fenland was briefly submerged by a proglacial palaeo-lake that formed at the margin of a glacier (Gibbard et al., 2018; West, 1993). Until ~8.2 kyr BP, the Fenland basin was connected with the European mainland by a land area called Doggerland (Coles, 1998) and then subsequently separated due to a sudden release of fresh water (Hijma and Cohen, 2010) and the Storegga slide tsunami (Weninger et al., 2008) that flooded Doggerland (Sturt et al., 2013). The evolution of Fenland topography during the Holocene was determined by competing rates of eustatic sea-level rise and sediment accumulation (Shennan et al., 2000; Waller, 1994). Further topographic modification likely emerged from the counteracting effects of isostatic rebound and crustal subsidence (Gibbard et al., 2018; Shennan and Horton, 2002). As the sea-level of the North Sea rose with varying rates in response to meltwater influxes, the groundwater table in the Fenland similarly fluctuated (Shennan et al., 2006, 2018). When submerged, silt, clay, and peat were accumulating (Brew et al., 2015; Waller and Kirby, 2021). When the rate of sedimentation exceeded the rate of sea-level rise, the coastline advanced seawards. However, this process was not homogeneous across the Fenland as meandering rivers and tides affected the distribution of land and water (Waller, 1994). By the 17th century CE, the Fenland was composed of 20-m thick waterlogged peat deposits, which were subsequently drained for farming (Smith et al., 2010). Although facilitating agriculture, the intensive drainage accelerated peat loss (Hutchinson, 1980), and the massive peat layer shrunk to an average thickness of 1.5 m (Holman, 2009). Annual ploughing of fields together with wind erosion continue to degrade the Fenland peat layer, and farmers frequently find subfossil tree trunks in their fields (Coles and Hall, 1997; Godwin, 1978; Miller and Skertchley, 1878; Waller, 1994). While most of the excavated subfossil wood in the Fenland has been described as "bog oaks" by farmers and subsequently used for dendrochronological research (Brown and Baillie, 1992), other species, including yew, have not yet been collected and analysed systematically. Although yew wood has not received much attention in dendrochronological research (there are only 12 published yew chronologies worldwide), there are a few studies on living yew trees from southern England (Hindson and Moir, 2023; Moir, 1999, 2004, 2021), which outline the species' dendrochronological potential.

Here, we present a collection of more than 400 subfossil yew trees from the Fenland basin in eastern England. We describe the morphological characteristics of our wood samples and discuss the environmental context in which the trees have been excavated. We use a combination of dendrochronological and radiocarbon dating to develop provisionally dated floating TRW chronologies. The new subfossil yew record is compared against independent proxy evidence of sea-level changes and pollen compositions. Finally, we place our findings in the context of putative climate trends and extremes in the mid-Holocene.

## 2. Data and methods

Following an extensive survey of Fenland farms, we identified 17 of them (labelled according to the geographical direction and farm name) with extensive piles of excavated subfossil wood (Fig. 1A). Nine farms are in the western (W: BF, EF, F1, F2, JF, LB, MF, RM, RF), four in the northern (N: BB, DF, DS, LF), three in the southern (S: GF, GS, RP), and

one in the eastern (E: HL) Fenland. We identified the wood species by macroscopic and microscopic observations (Ruffinato and Crivellaro, 2019). A distinct colour difference between heartwood and sapwood, a lack of resin canals, and helical thickening of axial tracheids refer to yew (*Taxus baccata* L.) (Schweingruber, 1978), whereas ring-porosity, large rays, and dendritic appearance of latewood vessels refer to oak (*Quercus* spp.). We collected 5 cm thick disc samples from 415 subfossil yew trees from 13 sites (Table 1). The well-preserved yew trunks are between two and eight metres long, and up to 60 cm thick in diameter (Figs. 1D and 2). With 90%, most of the trunks still contained a flat-root bowl, and circa 10% of the trunks exhibited well-defined layers of adventitious roots, which is a dendro-physiological indicator for sedimentation (Strunk, 1997), that spread horizontally with up to 30 cm between the layers (Fig. 2).

After visual inspection, short samples with less than 50 rings and decayed samples were excluded, and 223 discs were further prepared to a highly polished surface with up to 800-grit grain size sandpapers. TRW was measured at 0.001 mm precision using a Velmex™ measuring system and MeasureJ2X software (Voorhis and Krusic, 2006) along 2–5 straight radii, avoiding extreme widening and narrowing of the rings. TRW measurements were visually and statistically cross-dated in TSAPWin, CDendro, and COFECHA (Holmes, 1983; Rinn, 1996; Stokes, 1996). A new network-based (Phillips et al., 2015) visualisation technique was developed and applied to further facilitate cross-dating of our subfossil samples (Fig. S1). This method not only helps to detect trees that were growing simultaneously, but also highlights clusters of TRW series that cross-date well amongst themselves but fall into different time periods. Due to the irregular growth of yew (Thomas and Polwart, 2003), all TRW radii and all possible combinations of averaged TRW radii were considered independently for cross-dating. Furthermore, some TRW measurement series were trimmed in their beginning and/or at their end by up to 20% of their total lengths to further increase the common signal in the mean record. For chronology development, each tree was represented by an average of 1–5 TRW measurement series, detrended with a Friedman's super smooth function set to alpha equals 5 using ARSTAN (Cook et al., 2017), and plotted with the dplR package (Bunn, 2008) in R Studio. Floating yew TRW chronologies were compared with two absolutely dated oak and pine TRW chronologies from eastern England (Baillie and Brown, 1988; Boswijk and Whitehouse, 2002).

Radiocarbon ( $^{14}\text{C}$ ) dating was performed to provisionally date the dendro material (Pearson et al., 2022; Stuiver et al., 1998), and we therefore selected 50 yew discs that contained over 150 rings each, were not rotten or stained, exhibited relatively wide rings, and represented the spatial distribution of our sampling sites. All  $^{14}\text{C}$  measurements were performed by high precision 'MiniCarbonDatingSystem' (MICADAS)  $^{14}\text{C}$  Accelerator Mass Spectrometers (AMS) in Manheim (Germany) and Zurich (Switzerland). Since both AMS facilities require only 20 mg of organic material (Synal et al., 2007), we were able to process the cellulose from individual tree rings via the base-acid-base-acid method (Nèmec et al., 2010), followed by bleaching and graphitising (Wacker et al., 2010). Single tree rings from 38 discs were dated in Germany, and blocks of 10–30 rings from 12 discs were dated in Switzerland. In addition, 12 discs out of a total of 50 were sampled twice, once from near the centre of the discs and once from near the outer edge of the disc, with a known number of rings between, to improve final wiggle-matching (Bronk Ramsey et al., 2001) against the Northern Hemisphere calibration curve IntCal20 (Reimer et al., 2020). A duplicate sample from one disc was sent to both laboratories for cross-validation. All 63  $^{14}\text{C}$  dates were statistically resolved in the OxCal v.4.4 software (Bronk Ramsey, 1995, 2021).

The tree-ring data were compared with two other types of palaeoenvironmental proxy archives; *Taxus* pollen records from the Fenland (Waller, 1994), and marine index points used for the reconstruction of sea-level changes in the North Sea (Brew et al., 2000; Shennan et al., 2018; Waller, 1994) (Fig. 1). Since the published radiocarbon dates of

**Table 1**  
Subfossil wood sites.

Code	Site	Coordinates N	Coordinates E	Oak trunks	Yew trunks	Collected yew trunks
W:BF	Burges&Sons Farm	52.50452	-0.12783	0	15	4
W:EF	Elm Farm	52.76364	-0.33066	20	5	2
W:F1	South Fen	52.78649	-0.31209	10	400	209
W:F2	South Fen	52.78649	-0.31209	0	100	31
W:JF	Johnatan's Farm	52.46735	-0.1993	100	0	0
W:LB	Leverton Brothers Farm	52.79597	-0.31916	0	100	76
W:MF	Mason Farm	52.77411	-0.34286	0	50	38
W:RF	Ramsey Height Farm	52.45486	-0.14305	100	3	3
W:RM	Ramsey Mike	52.46056	-0.17778	100	0	0
N:BB	Bardney Bridge	53.20792	-0.3419	20	2	2
N:DF	Dyson Farming	53.1875	-0.33358	100	10	9
N:DS	Deaton&Sons	53.20575	-0.35429	20	2	2
N:LF	Lock Farm	53.21667	-0.35315	15	0	0
S:GF	Glover Farm	52.41774	0.433259	5	3	0
S:GS	GS Fresh	52.3557	0.293965	30	0	0
S:RP	Road pile	52.42444	0.431455	5	40	35
E:HL	Hamish Low	52.53647	0.457179	1	3	4

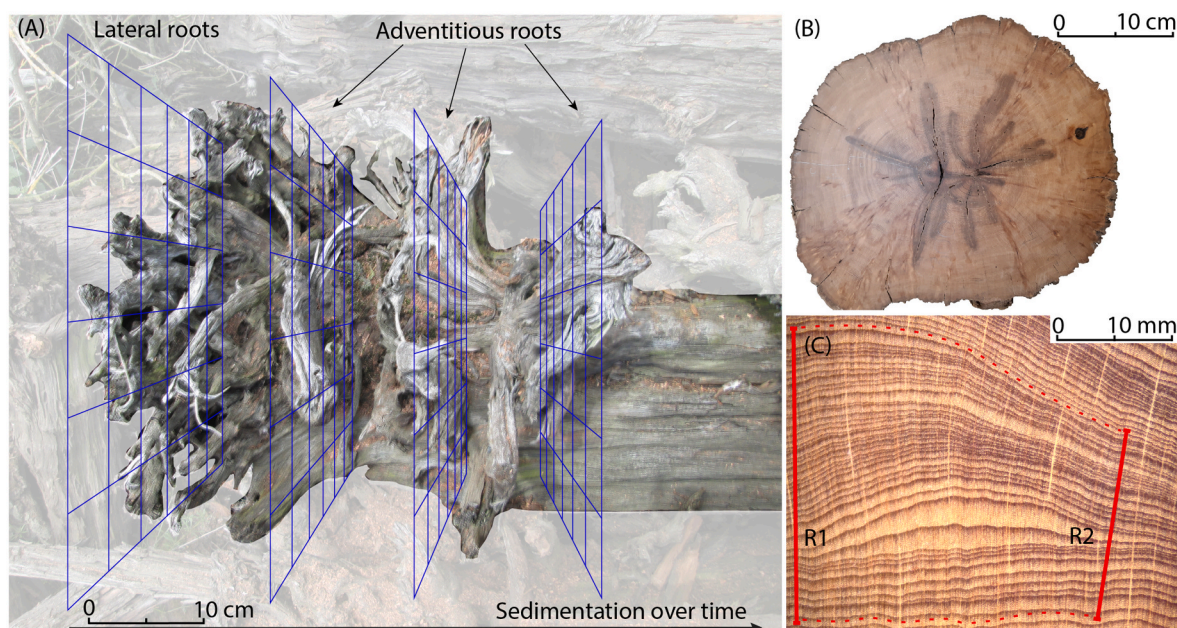


**Fig. 2.** (A) Yew trunk exhibiting three layers of adventitious roots with ~10 cm in between. The blue planes highlight horizontal spreading of the roots. (B) Subfossil yew disc including cracks, originating from the pith, black stain along the cracks, compression wood near the centre, and epicormic buds (knots). (C) Tree rings of a yew disc with high number of locally absent rings. Note that counting the rings along the red radius R1 gives 42 rings between the dotted rings, while along the blue radius R2, there are 29 rings only.

these records were originally calibrated using older radiocarbon calibration curves, causing issues for comparisons, we have recalibrated all  $^{14}\text{C}$  dates using the Bayesian models in OxCal v4.4.4 (Bronk Ramsey, 2009, 2021) and the IntCal20 calibration curve (Reimer et al., 2020). Following the protocols outlined in Lowe et al. (2019) and Lincoln et al. (2020) two types of the Bayesian models were employed, P\_Sequence and U\_Sequence models (Table S2), to remodel the previously published radiocarbon dates.

### 3. Results

All the yew samples from across the Fenland, except those from a southern site S:RP, represent specimens of mature woodlands. Most of our yew discs contain 150–250 rings. The youngest (at S:RP) and oldest (at W:LB) samples contain 44 and 408 rings, respectively (Fig. 3). The number of rings per trunk at S:RP ( $n = 32$ ) ranges between 44 and 126, with a mean segment length (MSL) of 74. In contrast, sites in the western Fenland W:F1 ( $n = 66$ ), W:F2 ( $n = 20$ ), W:MF ( $n = 30$ ), and W:LB ( $n =$

59) only contain trees older than 70 years, and their MSLs range between 179 and 222 years. At every site, there are 1–4 individual trunks that exceed MSL by 2.5 standard deviations. The average growth rate (AGR) of the trees from the neighbouring sites (W:F1 and W:F2, and W:MF and W:LB) is equal, and overall AGR decreases from 0.84 in S:RP to 0.57 in W:LB (Fig. 3).

Radiocarbon dating helped anchor the material in time and revealed that yew was present in the Fenland between 5300 and 4000 years cal BP (Fig. 5A, Table S3). The temporal distribution of  $^{14}\text{C}$  dates is site-specific (Fig. 5A): the samples from W:LB ( $n = 14$ ), W:MF ( $n = 7$ ) and S:RP ( $n = 4$ ) fall between 5200 and 4900 years cal BP, whereas samples from W:F1 ( $n = 11$ ) and W:F2 ( $n = 3$ ) cover the period 4500–4200 years cal BP, and only five samples, two of which are from E:HL, bridge the gap between 4900 and 4500 years cal BP. Most of the  $^{14}\text{C}$  samples fall on plateaux in the IntCal20 calibration curve (Fig. S2), resulting in dating uncertainties of  $\pm 10$  to  $\pm 101$  years, on average  $\pm 57$  years. Wiggle-matching two samples from the same disc reduced the uncertainty to  $\pm 36$  years on average. The reduction of temporal uncertainty was higher

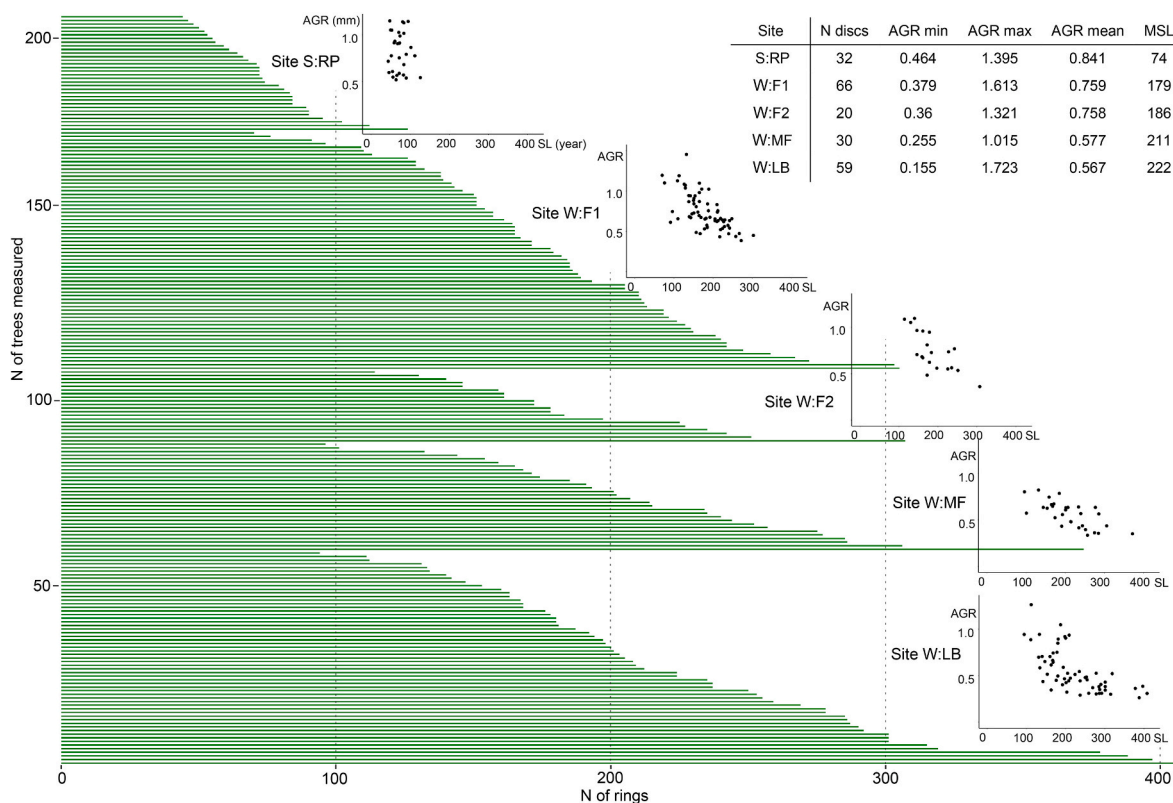


**Fig. 3.** Age distribution of the yew discs at five sites with the largest number of subfossil yew wood. Trees are grouped by sites and sorted by the number of rings exhibited on the discs. The scatter plots show the relation between segment length (SL, years) and average growth rate (AGR, mm) per site, after Esper et al. (2003).

when the number of rings (i.e. years) between the samples from an inner and an outer parts of a disc was large (Fig. S3), albeit it depends on the precision and configuration of the radiocarbon calibration curve. For example, a distance of 138 rings enabled us to reduce the uncertainty from  $\pm 85$  to  $\pm 41$  years, whereas a distance of 45 years improved the uncertainty from  $\pm 47$  to  $\pm 38$  years.

Two yew floating chronologies, SW and W for the south-western and western Fenland, respectively, were developed and anchored in time (Table 3, Figs. 4 and 5B). The SW chronology includes 32 trees from the sites W:F1, W:F2, W:LB, W:MF, and S:RP, has a mean inter-series correlation of 0.5 and spans 413 years. Six trees with a total of 9  $^{14}\text{C}$  dates place the SW chronology between 5225 and  $4813 \pm 4$  years cal BP. The W chronology includes 36 trees from the sites W:F1 and W:F2, has a mean inter-series correlation of 0.51 and spans 418 years. Ten trees with a total of 13  $^{14}\text{C}$  dates place the W chronology between 4612 and  $4195 \pm 6$  years cal BP. As a result, the chronologies cover a millennium with a temporal gap of 200 years between 4813 and 4612 years cal BP. The attempt to cross-date both floating yew chronologies against absolutely dated oak and pine chronologies remained statistically uncertain.

Resolving the  $^{14}\text{C}$  dates of non-dendrochronological palaeoenvironmental proxy archives resulted in high temporal uncertainties.

**Table 2**

Characteristics of yew discs commonly encountered throughout the collection.

Wood characteristics	Percentage of the discs exhibiting the feature (%)
Star-shaped cracks	85
Compression wood at the juvenile stage only	10
Constant compression wood (oval-shape disc)	40
Epicormic buds	20
Local widening of the rings	35
Locally absent rings	>60

After recalibration of the *Taxus baccata* pollen records, the uncertainties range between  $\pm 41$  and  $\pm 751$  years with an average of  $\pm 154$  years (Fig. 5C). In Fig. 5C, the duration of *Taxus* is shown as an orange line between the dating of the *Taxus* pollen found in a core, together with the uncertainties associated with these dates. The youngest pollen grains tend to have higher dating uncertainties due to a lack of carbonaceous material above them that was radiocarbon dated. Recalibration of the  $^{14}\text{C}$  dates of the Fenland marine index points resulted in a temporal uncertainty between  $\pm 59$  and  $\pm 186$  years with an average of  $\pm 119$  years. In Fig. 5D, the temporal uncertainty of each point is shown, and the overall trend of a sea-level rise, with short fluctuations, is highlighted.

#### 4. Discussion

Despite the general high quality of subfossil yew wood, TRW measuring and cross-dating are complicated by the morphological characteristics of the discs and irregular pattern of yew ring formation (Table 2). Cracks with black-stained edges and epicormic buds obstruct the visibility of the rings. Locally extreme widening and narrowing of the rings results in high intra-annual variability of the ring widths. Hence, the inter-annual TRW variability is better captured when measuring TRWs along straight lines rather than along a meandering (or segmented) radius in order to avoid areas of narrow rings or decay. A large number of locally absent rings (up to 40 per disc) further complicates cross-dating.

The  $^{14}\text{C}$  dates play a vital role as they independently validate cross-dating results, ensuring that the cross-dated trees have grown simultaneously. Although IntCal20 resolution in the period of yew growth is 5–20 years (Reimer et al., 2020), wiggle-matching radiocarbon dates enabled placing the tree-ring data in time with sufficient precision to enable refinement of other palaeoenvironmental proxies and reconstruction of the climatic and environmental changes.

**Table 3**  
Statistics of yew floating TRW chronologies.

Chronology code (site source)	N of trees	<sup>14</sup> C dated trees (measurements)	Length, years	Dates, cal BP	Uncertainty, ±years	Inter-series correlation	AGR	MSL
SW (W:F1, F2, LB, MF, S:RP)	36	10(13)	413	5225–4813	4	0.50	0.68	165
W (F1, F2)	32	6(9)	418	4612–4195	6	0.51	0.73	183

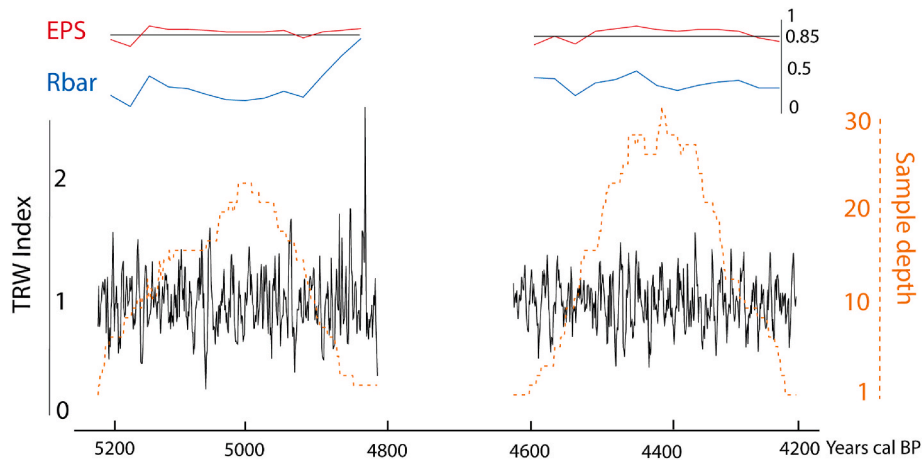


**Fig. 4.** Provisionally dated total ring-width chronologies, SW (on the left) and W (on the right) with their sample depth, expressed population signal (EPS) and Rbar.

Our yew tree-ring data exhibit low inter-series correlations of 0.45–0.55 indicating that a potential climate signal, if present in the chronologies, is limited in strength. This is likely due to the yews not growing in an environment with pronounced temperature or hydro-climate limitations, which consequently limits our ability to infer from these chronologies climate changes at high resolution. However, our yew records do provide high-resolution dating of changes in the environment that affect tree growth rates, presence and absence, and shifts in preservation conditions.

Our tree-ring data reveal that the yew trees colonised the southern (S:RP) and western (W:LB, MF) parts of the Fenland at ~5250 years cal BP (Fig. 5A and B). This timing coincides with the earliest pollen evidence of *Taxus* in the Fenland (Fig. 5C), which was found at Peacock's Farm (Waller, 1994) and dated to  $5200 \pm 100$  years cal BP after recalibrating with IntCal20 (Reimer et al., 2020). Furthermore, the onset of the yew tree-ring data matches the hypothesis that yew expansion in England followed the elm decline after ~5300 years cal BP (Batchelor et al., 2020; Bennett, 1988; Mitchell, 1990; Parker et al., 2002; Peglar and Birks, 1993; Waller, 1994; Waller and Early, 2015). In the south, (S:RP) yew disappeared by ~5000 years cal BP, whereas in the western sites (W:LB, MF) yew formed climax pure woodlands with individual trees over 400 years old till ~4800 years cal BP. Between 4800 and 4600 years cal BP, little evidence of yew is derived only from the eastern (E:HL) part of the Fenland. These temporal yew declines at ~4700 years cal BP are also demarcated in the pollen records at Hobhole A, Lade Bank, Hobbs Lot March, and Ouse Hadenham (Waller, 1994) (Fig. 5C). The second period of abundant yew growth began around 4600 years cal BP. Yew trees colonised western (W:BF, F1, F2, RF) sites ~4550 years cal BP, and northern (N:BB, DF, DS) part of the Fenland was colonised ~4450 years cal BP. At all localities, yew disappeared around 4200 years cal BP. Such an abrupt shift in species' abundance could be the result of either a decline of yew trees or changes in preservation conditions. In the pollen records (Waller, 1994), the decline of *Taxus* is not abrupt but spread out over time (Fig. 5C). However, we acknowledge there are issues with the dating resolution of these pollen records, many of which have used linear interpolation to extend their chronologies resulting in uncertainties of up to  $\pm 750$  years. Irrespective of their dating uncertainties, these pollen records provide independent evidence

for the yew disappearance in the Fenland.

The spatial distribution (Fig. 1A) and morphological characteristics (Table 2) of the subfossil yew wood indicate the conditions of yew growth, death and subsequent preservation (depicted in Fig. 6). All 17 sites with subfossil wood are located near the borders of the Fenland basin close to its surrounding upland, and no wood has been found in the central Fenland. This suggests that wood preservation was taking place along the edges of the basin, and possibly that yews and oaks were growing close to the source of freshwater and further from marine inundated areas. As sea-level of the North Sea rose, the areas close to the sea were submerged under salt water and the areas further inland were flooded with freshwater. Under prolonged fresh waterlogging, peat accumulated, and yews produced adventitious roots to reduce oxygen deprivation and improve the tree's stability. Yew saplings survived on wet peat as around 10% of all yew samples exhibit extreme reaction wood near the pith, suggesting soil instability during juvenile growth. Despite these physiological adaptation mechanisms, even for peatbog trees, extreme water table heights can be a limiting factor (Eckstein et al., 2009; Edvardsson et al., 2012b; Leuschner et al., 2002; Sass-Klaassen and Hanraets, 2006; Turney et al., 2005). We therefore argue that yew experienced a temporal decline from ~4800 till ~4600 years cal BP as a result of a rising groundwater table that was a consequence of either general wetter climate conditions or the rise of relative sea-level (RSL). The latter would impact the basin directly in the north, and indirectly through the basin's drainage system. The sudden disappearance of yew woodlands ~4200 years cal BP, after which the species did not recover in the Fenland till present times (or at least neither wood nor pollen was preserved), suggests that more severe damage was done. We propose that a rapid sea-level rise, resulting in marine inundation, contributed to the ultimate yew loss due to the species' intolerance to salt water and salt aerosols (Thomas and Polwart, 2003). Shennan et al. (2018) date the largest extent of marine inundation to  $\sim 4500\text{--}4200 \pm 120$  years cal BP, when the entire Fenland basin was submerged. Recalibrated data of marine index reveal an increased rate of sea-level rise at  $4250 \pm 112$  years cal BP and a consequent peak of RSL at  $4200 \pm 112$  years cal BP.

The mid-Holocene yew decline has also been reported from pollen records across western coastal Europe. In Belgium, Deforce and

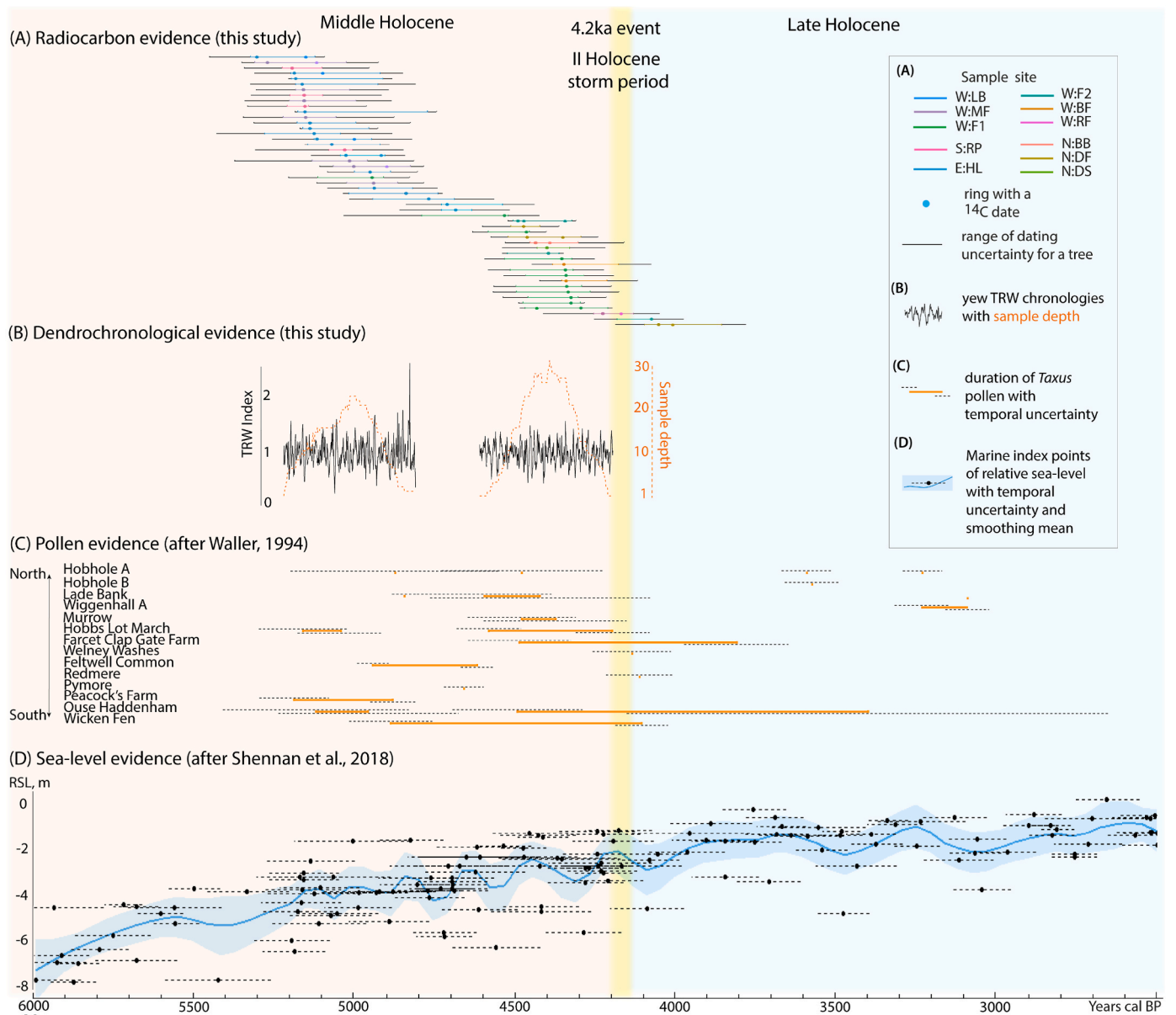


**Fig. 5.** (A) Radiocarbon dated yew disc samples. Each line represents a disc, and the colour indicates the site. The length of the colourful line is the number of rings measured on a disc. The black lines on both sides of the colourful line show the dating uncertainty for a tree, i.e. the period when the tree could have been growing. The dot marks the ring that was radiocarbon dated or the middle ring of a block that was dated (Table S3). (B) Yew TRW ARSTAN chronologies developed in this study with the sample depth (orange dashed line) and expressed population signal (EPS) relative to the accepted threshold of 0.85 (Wigley et al., 1984). (C) The duration of *Taxus baccata* pollen with an uncertainty, after Waller (1994). The  $^{14}\text{C}$  dates were recalibrated with IntCal20 (Reimer et al., 2020) using the age-depth model function in OxCal (Bronk Ramsey, 2021). Note that the length of the line (i.e. duration) is not rigid. (D) Reconstruction of relative sea-level (RSL, m) changes in the Fenland, after Shennan et al. (2018). The  $^{14}\text{C}$  dates were taken from Waller (1994) and recalibrated with IntCal-20. The Middle Holocene and Late Holocene epochs are marked (Walker et al., 2014), and the 4.2 ka event (Walker et al., 2019) and the II Holocene storm period (Sorrel et al., 2012) are highlighted in yellow. Colours must be used in print.

Bastiaens (2007) found yew declined around 3500 BP; whilst in England, Wheeler (1992) dates the species decline at 3600 BP, Batchelor et al. (2020) at 4000 and Bennett (1988) at 4200 BP. Moreover, sudden reductions in the population of dendrochronologically dated pines and oaks that also colonised peatlands, occurred between 4250 and 4120 calendar years BP in eastern England (Baillie and Brown, 1988), Ireland (Turney et al., 2005), the Netherlands (Leuschner et al., 2002), and Germany (Eckstein et al., 2010, 2011; Leuschner et al., 2000).

The yew decline in the Fenland coincides with the so-called “4.2ka-event” (Bond Event 3; Bond et al., 2001) (Fig. 5). This event is attributed to the abrupt global climate changes at 4200–3900 years BP (Walker et al., 2014). Despite the fact that the causes of this event remain unclear

(Toth and Aronson, 2019), it has become adopted as the formally defined boundary between the Middle Holocene and Late Holocene Subseries (Walker et al., 2019). In the North Atlantic, Mayewski et al. (2004) found that westerly winds were exceptionally strong during 4.2 ka, and Sorrel et al. (2012) identified a period 4.2–4.0 ka BP as the Second Holocene storm period based on the data from the North Sea. Both strong westerlies, increasing humidity and high storms would intensify yew mortality primarily through rapid sea-level rise.

## 5. Conclusion

This study presents two 400-year-long subfossil yew TRW

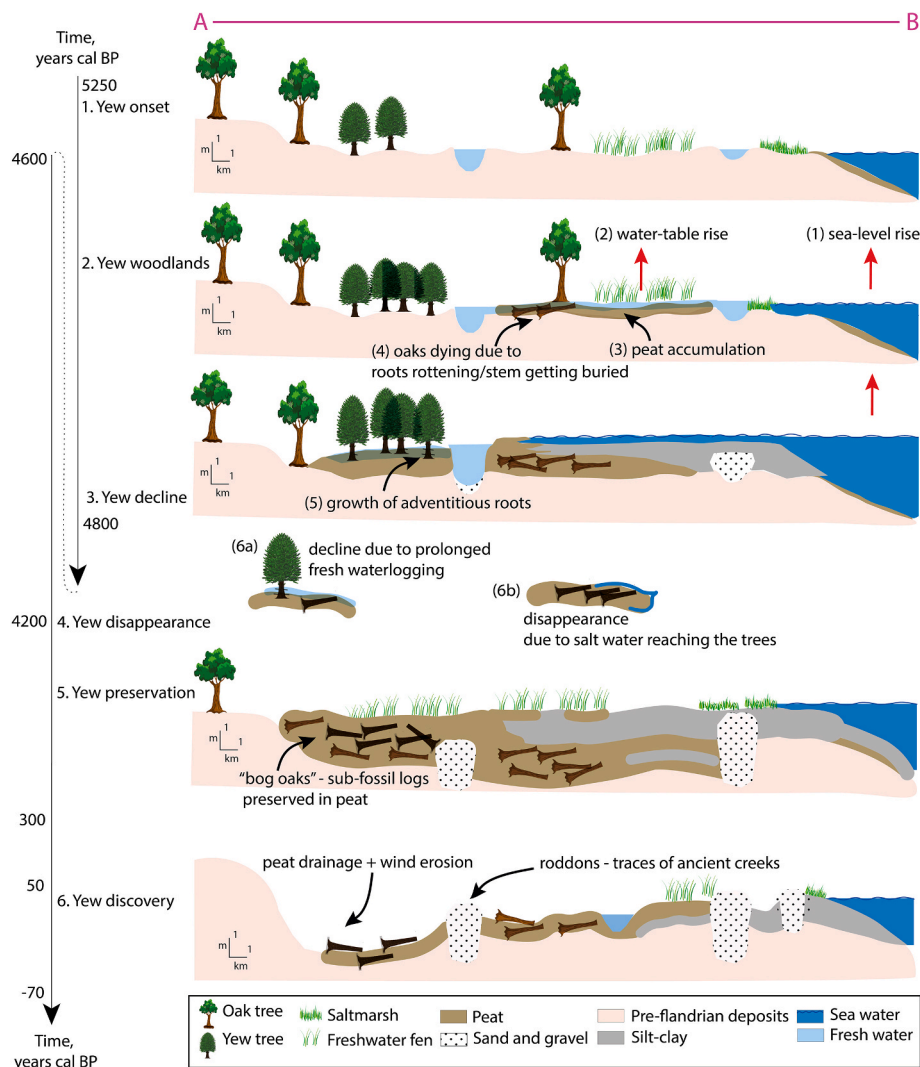


**Fig. 6.** Schematic depiction of the conditions of yew growth and decline regarding the environmental history of the Fenland in the mid- and late-Holocene. The profile A-B drawn through the Fenland is shown in Fig.1. Predominant environmental processes controlling yew growth are depicted: sea-level rise (1) leads to the increase of water-table (2), and under the fresh waterlogging conditions, peat accumulates (3). This leads to the lack of oxygen available for the roots, which in turn results in oak death (4) and the production of adventitious roots by yew trees (5). The eventual yew death is caused by either (6a) prolonged waterlogging conditions, or (6b) saltwater reaching yew trees due to the rapid sea-level rise. Finally, the stages of the Fenland topography over the last centuries are shown. *Colours must be used in print.*

chronologies that span between 5225 and  $4813 \pm 4$  and between  $4612$  and  $4195 \pm 6$  years cal BP. Our study highlights the rapid expansion ( $\sim 5200$ ), temporal decline ( $\sim 4700$ ) and final disappearance ( $\sim 4200$ ) of *Taxus* in the Fenland, and sheds new light on the possible impact of the putative 4.2 ka climate event on NW Europe. Our new yew TRW chronologies can facilitate the dating of archaeological remnants and once absolutely dated, can be used for improving the resolution of the international radiocarbon calibration curve IntCal (Reimer et al., 2020). To enable climate interpretation and to critically assess if the disappearance of yew woodlands in eastern England was caused by marine inundation, annually resolved stable isotope analyses are needed. Our study also recognises the fragility of this proxy archive, which may vanish in the years to come once the subfossil material is exhumed and exposed to air.

#### Author contribution

Tatiana Bebchuk: Conceptualization, Methodology, Software, Formal analysis, fieldwork, TRW measurements, Visualisation, writing an original draft and editing it; Paul J. Krusic and Joshua H. Pike:

Software, Formal analysis, fieldwork, editing final draft; Alma Piermattei: Formal analysis, fieldwork, editing final draft, Ronny Friedrich: radiocarbon dating; Lukas Wacker: radiocarbon dating; Alan Crivellaro, Tito Arosio and Alexander V. Kiryanov: fieldwork, editing final draft; Philip Gibbard: Conceptualization, editing final draft; David Brown: Resources, editing final draft; Jan Esper and Frederick Reinig: editing final draft; Ulf Büntgen: Conceptualization, Methodology, fieldwork, writing an original draft and editing it, Project administration.

#### Declaration of competing interest

The authors declare that they have no known competing financial interests or personal relationships that could have appeared to influence the work reported in this paper.

#### Data availability

Data will be made available on request.



## Acknowledgements

TB was funded by the Hill Foundation Cambridge Trust. TA is supported by SNSF P500PN\_210716. We would like to thank Hermione Wright for the assistance in measuring TRW, Victor Souza for the idea to use network principals in the cross-dating procedure, and Hamish Low and the various landowners who granted access to collect the tree-ring samples.

## Appendix A. Supplementary data

Supplementary data to this article can be found online at <https://doi.org/10.1016/j.quascirev.2023.108414>.

## References

- Allen, K.J., Cook, E.R., Buckley, B.M., Larsen, S.H., Drew, D.M., Downes, G.M., Francey, R.J., Peterson, M.J., Baker, P.J., 2014. Continuing upward trend in Mt Read Huon pine ring widths – temperature or divergence? *Quat. Sci. Rev.* 102, 39–53. <https://doi.org/10.1016/j.quascirev.2014.08.003>.
- Baillie, M.G.L., Brown, D.M., 1988. An overview of oak chronologies. In: *Science and Archaeology. Presented at the Science and Archaeology. B.A.R. British Series 196, Glasgow, 1987*.
- Batchelor, C.R., Branch, N.P., Carew, T., Elias, S.E., Gale, R., Lafferty, G.E., Matthews, I. P., Meddens, F., Vaughan-Williams, A., Webster, L.A., Young, D.S., 2020. Middle-Holocene environmental change and archaeology in coastal wetlands: further implications for our understanding of the history of Taxus woodland. *Holocene* 30, 300–314. <https://doi.org/10.1177/0959683619883028>.
- Bennett, K.D., 1988. Holocene pollen stratigraphy of central East Anglia, England, and comparison of pollen zones across the British Isles. *New Phytol.* 109, 237–253. <https://doi.org/10.1111/j.1469-8137.1988.tb03712.x>.
- Biondi, F., Meko, D.M., Piovessan, G., 2023. Maximum tree lifespans derived from public-domain dendrochronological data. *iScience* 26, 106138. <https://doi.org/10.1016/j.isci.2023.106138>.
- Bond, G., Kromer, B., Beer, J., Muscheler, R., Evans, M.N., Showers, W., Hoffmann, S., Lotti-Bond, R., Hajdas, I., Bonani, G., 2001. Persistent solar influence on North Atlantic climate during the Holocene. *Science* 294, 2130–2136. <https://doi.org/10.1126/science.1065680>.
- Boswijk, G., Whitehouse, N.J., 2002. Pinus and Proximos: a dendrochronological and palaeontological study of a mid-Holocene woodland in eastern England. *Holocene* 12, 585–596. <https://doi.org/10.1191/0959683602hl569rp>.
- Brew, D., Holt, T., Pye, K., Newsham, R., 2000. Holocene sedimentary evolution and palaeocoastlines of the Fenland embayment, eastern England. Geological Society, London, Special Publications 166, 253–273. <https://doi.org/10.1144/GSL.SP.2000.166.01.13>.
- Brew, D.S., Horton, B.P., Evans, G., Innes, J.B., Shennan, I., 2015. Holocene sea-level history and coastal evolution of the north-western Fenland, eastern England. *PGA (Proc. Geol. Assoc.)* 126, 72–85. <https://doi.org/10.1016/j.pgeola.2014.12.001>.
- Bronk Ramsey, C., 2021. OxCal v4. 4.4. Available at: Retrieved from. <https://c14.arch.ox.ac.uk/oxcal.html>.
- Bronk Ramsey, C., 2009. Bayesian analysis of radiocarbon dates. *Radiocarbon* 51, 337–360. <https://doi.org/10.1017/S0033822200033865>.
- Bronk Ramsey, C., Plicht, J. van der, Weninger, B., 2001. ‘Wiggle matching’ radiocarbon dates. *Radiocarbon* 43, 381–389. <https://doi.org/10.1017/S0033822200038248>.
- Brown, D.M., Baillie, M.G.L., 1992. Construction and dating of a 5000 Year English bog oak tree-ring chronology. *Tree ring and environment. In: Proceedings of the International Dendrochronological Symposium*.
- Bunn, A.G., 2008. A dendrochronology program library in R (dplR). *Dendrochronologia* 26, 115–124. <https://doi.org/10.1016/j.dendro.2008.01.002>.
- Büntgen, U., Arseneault, D., Boucher, É., Churakova (Sidorova), O.V., Gennaretti, F., Crivellaro, A., Hughes, M.K., Kiryanov, A.V., Klippel, L., Krusic, P.J., Linderholm, H.W., Ljungqvist, F.C., Ludeschner, J., McCormick, M., Myglan, V.S., Nicolussi, K., Piermattei, A., Oppenheimer, C., Reinig, F., Sigl, M., Vaganov, E.A., Esper, J., 2022. Recognising bias in Common Era temperature reconstructions. *Dendrochronologia* 74, 125982. <https://doi.org/10.1016/j.dendro.2022.125982>.
- Christensen, K., 2007. Forhistorisk dendrokronologi i Danmark. *Kuml* 56, 217–236. <https://doi.org/10.7146/kuml.v56i56.24682>.
- Coles, B.J., 1998. Doggerland: a Speculative survey. *Proc. Prehist. Soc.* 64, 45–81. <https://doi.org/10.1017/S0079497X00002176>.
- Coles, J., Hall, D., 1997. The Fenland Project: from survey to management and beyond. *Antiquity* 71, 831–844. <https://doi.org/10.1017/S0003598X00085768>.
- Cook, E.R., Buckley, B.M., D’Arrigo, R.D., Peterson, M.J., 2000. Warm-season temperatures since 1600 BC reconstructed from Tasmanian tree rings and their relationship to large-scale sea surface temperature anomalies. *Clim. Dynam.* 16, 79–91. <https://doi.org/10.1007/s003820050006>.
- Cook, E.R., Krusic, P.J., Peters, K., Holmes, R.L., 2017. Program ARSTAN 49v1, Autoregressive Tree-Ring Standardization Program. Tree-Ring Laboratory of Lamont-Doherty Earth Observatory.
- Deforce, K., Bastiaens, J., 2007. The Holocene history of *Taxus baccata* (yew) in Belgium and neighbouring regions. *Belg. J. Bot.* 140, 222–237.
- Eckstein, J., Leuschner, H.H., Bauerochse, A., 2011. Mid-Holocene pine woodland phases and mire development – significance of dendroecological data from subfossil trees from northwest Germany. *J. Veg. Sci.* 22, 781–794. <https://doi.org/10.1111/j.1654-1103.2011.01283.x>.
- Eckstein, J., Leuschner, H.H., Bauerochse, A., Sass-Klaassen, U., 2009. Subfossil bog-pine horizons document climate and ecosystem changes during the Mid-Holocene. *Dendrochronologia, EuroDendro 2008: The long history of wood utilization* 27, 129–146. <https://doi.org/10.1016/j.dendro.2009.06.007>.
- Eckstein, J., Leuschner, H.H., Giesecke, T., Shumilovskikh, L., Bauerochse, A., 2010. Dendroecological investigations at Venner Moor (northwest Germany) document climate-driven woodland dynamics and mire development in the period 2450–2050 BC. *Holocene* 20, 231–244. <https://doi.org/10.1177/0959683609350397>.
- Edvardsson, J., Leuschner, H.H., Linderson, H., Linderholm, H.W., Hammarlund, D., 2012a. South Swedish bog pines as indicators of Mid-Holocene climate variability. *Dendrochronologia, WORLD DENDRO 2010* (30), 93–103. <https://doi.org/10.1016/j.dendro.2011.02.003>.
- Edvardsson, J., Linderson, H., Rundgren, M., Hammarlund, D., 2012b. Holocene peatland development and hydrological variability inferred from bog-pine dendrochronology and peat stratigraphy – a case study from southern Sweden. *J. Quat. Sci.* 27, 553–563. <https://doi.org/10.1002/jqs.2543>.
- Edvardsson, J., Stoffel, M., Corona, C., Bragazza, L., Leuschner, H.H., Charman, D.J., Helama, S., 2016. Subfossil peatland trees as proxies for Holocene palaeohydrology and palaeoclimate. *Earth Sci. Rev.* 163, 118–140. <https://doi.org/10.1016/j.earscirev.2016.10.005>.
- Esper, J., Cook, E.R., Krusic, P.J., Peters, K., Schweingruber, F.H., 2003. Tests of the RCS method for preserving low-frequency variability in long tree-ring chronologies. *Tree-Ring Res.* 59, 81–98.
- Esper, J., Krusic, P.J., Ljungqvist, F.C., Luterbacher, J., Carrer, M., Cook, E., Davi, N.K., Hartl-Meier, C., Kiryanov, A., Konter, O., Myglan, V., Timonen, M., Treydte, K., Trouet, V., Villalba, R., Yang, B., Büntgen, U., 2016. Ranking of tree-ring based temperature reconstructions of the past millennium. *Quat. Sci. Rev.* 145, 134–151. <https://doi.org/10.1016/j.quascirev.2016.05.009>.
- Ferguson, C.W., 1969. A 7104-Year Annual Tree-Ring Chronology for Bristlecone Pine, *Pinus Aristata*, from the White Mountains, California.
- Ferguson, C.W., Graybill, D.A., 1983. Dendrochronology of bristlecone pine: a progress report. *Radiocarbon* 25, 287–288. <https://doi.org/10.1017/S0033822200005592>.
- Ferguson, C.W., Schulman, E., Fritts, H.C., 2002. NOAA/WDS Paleoclimatology - Ferguson - White Mountains Master - PILO - ITRDB CA506. <https://doi.org/10.25921/T59Z-Z509>.
- Friedrich, M., Remmele, S., Kromer, B., Hofmann, J., Spurk, M., Kaiser, K., Orצל, C., Küppers, M., 2004. The 12,460-year Hohenheim oak and pine tree-ring chronology from Central Europe; A unique annual record for radiocarbon calibration and paleoenvironment reconstructions. *Radiocarbon* 46, 1111–1122. [https://doi.org/10.2458/azu\\_js\\_rc.46.4172](https://doi.org/10.2458/azu_js_rc.46.4172).
- Fritts, H., 1976. *Tree Rings and Climate*.
- Gibbard, P.L., Bateman, M.D., Leathard, J., West, R.G., 2021. Luminescence dating of a late Middle Pleistocene glacial advance in eastern England. *Neth. J. Geosci.* 100, e18. <https://doi.org/10.1017/njg.2021.13>.
- Gibbard, P.L., West, R.G., Hughes, P.D., 2018. Pleistocene glaciation of Fenland, England, and its implications for evolution of the region. *R. Soc. Open Sci.* 5, 170736. <https://doi.org/10.1098/rsos.170736>.
- Godwin, H., 1978. *Fenland: its Ancient Past and Uncertain Future*. Cambridge University Press.
- Graybill, D.A., 2002. NOAA/WDS Paleoclimatology - Graybill - Methuselah Walk - PILO - ITRDB CA535. <https://doi.org/10.25921/PPQJ-XV48>.
- Graybill, D.A., 1996. NOAA/WDS Paleoclimatology - Graybill - Indian Garden - PILO - ITRDB NV515. <https://doi.org/10.25921/R81R-SW85>.
- Grudd, H., Briffa, K.R., Karlén, W., Bartholin, T.S., Jones, P.D., Kromer, B., 2002. A 7400-year tree-ring chronology in northern Swedish Lapland: natural climatic variability expressed on annual to millennial timescales. *Holocene* 12, 657–665. <https://doi.org/10.1191/0959683602hl578rp>.
- Hantemirov, R.M., Shiyatov, S.G., Gorlanova, L.A., Kukarskih, V.V., Surkov, A.Yu, Hamzin, I.R., Fonti, P., Wacker, L., 2021. An 8768-year Yamal tree-ring chronology as a tool for paleoecological reconstructions. *Russ. J. Ecol.* 52, 419–427. <https://doi.org/10.1134/S1067413621050088>.
- Helama, S., Mielikäinen, K., Timonen, M., Eronen, M., 2008. Finnish supra-long tree-ring chronology extended to 5634 BC. *Norsk Geografisk Tidsskrift - Norwegian Journal of Geography* 62, 271–277. <https://doi.org/10.1080/00291950802517593>.
- Hijma, M.P., Cohen, K.M., 2010. Timing and magnitude of the sea-level jump prelude the 8200 yr event. *Geology* 38, 275–278. <https://doi.org/10.1130/G30439.1>.
- Hindson, T.R., Moir, A.K., 2023. The dendrochronological potential of decayed yew wood. *Dendrochronologia* 79, 126087. <https://doi.org/10.1016/j.dendro.2023.126087>.
- Holman, I.P., 2009. An Estimate of Peat Reserves and Losses in the East Anglian Fens Commissioned by the RSPB. Department of Natural Resources Cranfield University, Cranfield, Bedfordshire.
- Holmes, R.L., 1983. Computer-assisted quality control in tree-ring dating and measurement. *Tree-Ring Bull.* 43.
- Hughes, P.D., Gibbard, P.L., 2015. A stratigraphical basis for the last glacial Maximum (LGM). *Quaternary International, The Quaternary System and its formal subdivision* 383, 174–185. <https://doi.org/10.1016/j.quaint.2014.06.006>.
- Hutchinson, J.N., 1980. The record of peat wastage in the East Anglian fenlands at Holme Post, 1848-1978 AD. *J. Ecol.* 68, 229–249.
- Lara, A., Villalba, R., Urrutia-Jalabert, R., González-Reyes, A., Aravena, J.C., Luckman, B. H., Cuq, E., Rodríguez, C., Wolodarsky-Franke, A., 2020. +A 5680-year tree-ring

- temperature record for southern South America. *Quat. Sci. Rev.* 228, 106087 <https://doi.org/10.1016/j.quascirev.2019.106087>.
- Leuschner, H.H., Sass-Klaassen, U., Jansma, E., Baillie, M.G.L., Spurk, M., 2002. Subfossil European bog oaks: population dynamics and long-term growth depressions as indicators of changes in the Holocene hydro-regime and climate. *Holocene* 12, 695–706. <https://doi.org/10.1191/0959683602h584rp>.
- Leuschner, H.H., Spurk, M., Baillie, M.G.L., Jansma, E., 2000. Stand dynamics of prehistoric oak forests derived from dendrochronologically dated subfossil trunks from bogs and riverine sediments in Europe. *Geolines* 11, 118–121.
- Lincoln, P.C., Matthews, I.P., Palmer, A.P., Blockley, S.P.E., Staff, R.A., Candy, I., 2020. Hydroclimatic changes in the British Isles through the last-glacial-Interglacial transition: multiproxy reconstructions from the vale of pickering, NE England. *Quat. Sci. Rev.* 249, 106630 <https://doi.org/10.1016/j.quascirev.2020.106630>.
- Ljungqvist, F.C., Piermattei, A., Seim, A., Krusic, P.J., Büntgen, U., He, M., Kiryanov, A. V., Luterbacher, J., Schneider, L., Seftigen, K., Stahle, D.W., Villalba, R., Yang, B., Esper, J., 2020. Ranking of tree-ring based hydroclimate reconstructions of the past millennium. *Quat. Sci. Rev.* 230, 106074 <https://doi.org/10.1016/j.quascirev.2019.106074>.
- Lowe, J., Matthews, I., Mayfield, R., Lincoln, P., Palmer, A., Staff, R., Timms, R., 2019. On the timing of retreat of the Loch Lomond (‘Younger Dryas’) readvance icefield in the SW Scottish highlands and its wider significance. *Quat. Sci. Rev.* 219, 171–186. <https://doi.org/10.1016/j.quascirev.2019.06.034>.
- Mayewski, P.A., Rohling, E.E., Stager, J.C., Karlén, W., Maasch, K.A., Meeker, L.D., Meyerson, E.A., Gasse, F., Kreveld, S. van, Holmgren, K., Lee-Thorp, J., Rosqvist, G., Roca, F., Staubwasser, M., Schneider, R.R., Steig, E.J., 2004. Holocene climate variability. *Quaternary Research* 62, 243–255. <https://doi.org/10.1016/j.yqres.2004.07.001>.
- Miller, S.H., Skertchley, S.B.J., 1878. *The Fenland Past and Present*.
- Mitchell, F.J.G., 1990. The history and vegetation dynamics of a yew wood (*Taxus baccata* L.) in S.W. Ireland. *New Phytol.* 115, 573–577. <https://doi.org/10.1111/j.1469-8137.1990.tb00486.x>.
- Moir, A., 2021. *Dendrochronological Analysis of a Yew Tree from St Mary's Churchyard, West Horsley, Surrey, England. Tree-Ring Services*.
- Moir, A., 2012. Development of a Neolithic pine tree-ring chronology for northern Scotland. *J. Quat. Sci.* 27, 503–508. <https://doi.org/10.1002/jqs.2539>.
- Moir, A.K., 2004. *Dendrochronological Analysis of a Yew Tree from St Marys Churchyard, vol. 20. West Horsley, Surrey, England*.
- Moir, A.K., 1999. The dendrochronological potential of modern yew (*Taxus baccata*) with special reference to yew from Hampton Court Palace, UK. *New Phytol.* 144, 479–488. <https://doi.org/10.1046/j.1469-8137.1999.00545.x>.
- Némec, M., Wacker, L., Hajdas, I., Gäggeler, H., 2010. Alternative methods for cellulose preparation for AMS measurement. *Radiocarbon* 52, 1358–1370. <https://doi.org/10.1017/S0033822200046440>.
- Nicolussi, K., Weber, G., Patzelt, G., Thurner, A., 2015. A Question of Time: Extension of the Eastern Alpine Conifer Chronology Back to 10071 B2k. *GFZ Potsdam, Scientific Technical Report STR15*. Potsdam, pp. 69–73. <https://doi.org/10.2312/GFZ.B103-15069>.
- Parker, A.G., Goudie, A.S., Anderson, D.E., Robinson, M.A., Bonsall, C., 2002. A review of the mid-Holocene elm decline in the British Isles. *Prog. Phys. Geogr. Earth Environ.* 26, 1–45. <https://doi.org/10.1191/0309133302pp323ra>.
- Pearson, C.L., Leavitt, S.W., Kromer, B., Solanki, S.K., Usoskin, I., 2022. Dendrochronology and radiocarbon dating. *Radiocarbon* 64, 569–588. <https://doi.org/10.1017/RDC.2021.97>.
- Peglar, S.M., Birks, H.J.B., 1993. The mid-Holocene Ulmus fall at Diss Mere, South-East England — disease and human impact? *Veget. Hist. Archaeobot.* 2, 61–68. <https://doi.org/10.1007/BF00202183>.
- Phillips, J.D., Schwanghart, W., Heckmann, T., 2015. Graph theory in the geosciences. *Earth Sci. Rev.* 143, 147–160. <https://doi.org/10.1016/j.earscirev.2015.02.002>.
- Pilcher, J.R., Baillie, M.G.L., Schmidt, B., Becker, B., 1984. A 7,272-year tree-ring chronology for western Europe. *Nature* 312, 150–152. <https://doi.org/10.1038/312150a0>.
- Ramsey, C.B., 1995. Radiocarbon calibration and analysis of stratigraphy: the OxCal program. *Radiocarbon* 37, 425–430. <https://doi.org/10.1017/S0033822200030903>.
- Reimer, P.J., Austin, W.E.N., Bard, E., Bayliss, A., Blackwell, P.G., Bronk Ramsey, C., Butzin, M., Cheng, H., Edwards, R.L., Friedrich, M., Grootes, P.M., Guilderson, T.P., Hajdas, I., Heaton, T.J., Hogg, A.G., Hughen, K.A., Kromer, B., Manning, S.W., Muscheler, R., Palmer, J.G., Pearson, C., van der Plicht, J., Reimer, R.W., Richards, D.A., Scott, E.M., Southon, J.R., Turney, C.S.M., Wacker, L., Adolph, F., Büntgen, U., Capano, M., Fahrni, S.M., Fogtmann-Schulz, A., Friedrich, R., Köhler, P., Kudsk, S., Miyake, F., Olsen, J., Reinig, F., Sakamoto, M., Sookdeo, A., Talamo, S., 2020. The IntCal20 northern Hemisphere radiocarbon age calibration curve (0–55 cal kBP). *Radiocarbon* 62, 725–757. <https://doi.org/10.1017/RDC.2020.41>.
- Rinn, F., 1996. *TSAP - Time Series Analyses Presentation. Referenz Manual (Version 3.0). RinnTech, Heidelberg*.
- Ruffinatto, F., Crivellaro, A., 2019. *Atlas of Macroscopic Wood Identification: with a Special Focus on Timbers Used in Europe and CITES-Listed Species*. Springer Nature.
- Salzer, M.W., 2010. NOAA/WDS Paleoclimatology - Salzer - Pearl Peak Update - PILO - ITRDB NV521. <https://doi.org/10.25921/RF2E-KB29>.
- Salzer, M.W., Hughes, M.K., 2010a. NOAA/WDS Paleoclimatology - Salzer - Mount Washington Nevada Update - PILO - ITRDB NV520. <https://doi.org/10.25921/21EW-PA87>.
- Salzer, M.W., Hughes, M.K., 2010b. NOAA/WDS Paleoclimatology - Salzer - Sheep Mountain Update - PILO - ITRDB CA667. <https://doi.org/10.25921/YCPW-7019>.
- Sass-Klaassen, U., Hanraets, E., 2006. Woodlands of the past—the excavation of wetland woods at Zwolle-Stadshagen (The Netherlands): growth pattern and population dynamics of oak and ash. *Neth. J. Geosci.* 85, 61–71.
- Schweingruber, F.H., 1978. *Microscopic Wood Anatomy*. Swiss Federal Institute of Forestry Research.
- Shennan, I., Bradley, S., Milne, G., Brooks, A., Bassett, S., Hamilton, S., 2006. Relative sea-level changes, glacial isostatic modelling and ice-sheet reconstructions from the British Isles since the Last Glacial Maximum. *J. Quat. Sci.* 21, 585–599. <https://doi.org/10.1002/jqs.1049>.
- Shennan, I., Bradley, S.L., Edwards, R., 2018. Relative sea-level changes and crustal movements in Britain and Ireland since the last glacial Maximum. *Quat. Sci. Rev.* 188, 143–159. <https://doi.org/10.1016/j.quascirev.2018.03.031>.
- Shennan, I., Horton, B., 2002. Holocene land- and sea-level changes in Great Britain. *J. Quat. Sci.* 17, 511–526. <https://doi.org/10.1002/jqs.710>.
- Shennan, I., Lambeck, K., Flather, R., Horton, B., McArthur, J., Innes, J., Lloyd, J., Rutherford, M., Wingfield, R., 2000. Modelling western North Sea palaeogeographies and tidal changes during the Holocene. Geological Society, London, Special Publications 166, 299–319. <https://doi.org/10.1144/GSL.SP.2000.166.01.15>.
- Smith, D.M., Zalasiewicz, J.A., Williams, M., Wilkinson, I.P., Redding, M., Begg, C., 2010. Holocene drainage systems of the English Fenland: roddons and their environmental significance. *PGA (Proc. Geol. Assoc.)* 121, 256–269. <https://doi.org/10.1016/j.pgeola.2010.06.002>.
- Sorrel, P., Debret, M., Billeaud, I., Jaccard, S.L., McManus, J.F., Tessier, B., 2012. Persistent non-solar forcing of Holocene storm dynamics in coastal sedimentary archives. *Nat. Geosci.* 5, 892–896. <https://doi.org/10.1038/ngeo1619>.
- Stokes, M.A., 1996. *An Introduction to Tree-Ring Dating*. University of Arizona Press.
- Strunk, H., 1997. Dating of geomorphological processes using dendrogeomorphological methods. *Catena* 31, 137–151. [https://doi.org/10.1016/S0341-8162\(97\)00031-3](https://doi.org/10.1016/S0341-8162(97)00031-3).
- Stuiver, M., Reimer, P.J., Bard, E., Beck, J.W., Burr, G.S., Hughen, K.A., Kromer, B., McCormac, G., Plicht, J.V.D., Spurk, M., 1998. INTCAL98 radiocarbon age calibration, 24,000–0 cal BP. *Radiocarbon* 40, 1041–1083. <https://doi.org/10.1017/S0033822200019123>.
- Sturt, F., Garrow, D., Bradley, S., 2013. New models of north west European Holocene palaeogeography and inundation. *J. Archaeol. Sci.* 40, 3963–3976. <https://doi.org/10.1016/j.jas.2013.05.023>.
- Synal, H.-A., Stocker, M., Suter, M., 2007. MICADAS: a new compact radiocarbon AMS system. *Nucl. Instrum. Methods Phys. Res., Sect. B: Beam Interactions with Materials and Atoms, Accelerator Mass Spectrometry* 259, 7–13. <https://doi.org/10.1016/j.nimb.2007.01.138>.
- Tegel, W., Muigg, B., Skiadas, G., Vanmoerkerke, J., Seim, A., 2022. *Dendroarchaeology in Europe*. Frontiers in Ecology and Evolution 10.
- Thomas, P.A., Polwart, A., 2003. *Taxus baccata* L. *J. Ecol.* 91, 489–524.
- Toth, L.T., Aronson, R.B., 2019. The 4.2 ka event, ENSO, and coral reef development. *Clim. Past* 15, 105–119. <https://doi.org/10.5194/cp-15-105-2019>.
- Turney, C., Baillie, M., Clemens, S., Brown, D., Palmer, J., Pilcher, J., Reimer, P., Leuschner, H.H., 2005. Testing solar forcing of pervasive Holocene climate cycles. *J. Quat. Sci.* 20, 511–518. <https://doi.org/10.1002/jqs.927>.
- Voorhis, N., Krusic, P.J., 2006. *Project J2X Tree-Ring Measuring Program*.
- Wacker, L., Bonani, G., Friedrich, M., Hajdas, I., Kromer, B., Némec, M., Ruff, M., Suter, M., Synal, H.-A., Vockenhuber, C., 2010. MICADAS: routine and high-precision radiocarbon dating. *Radiocarbon* 52, 252–262. <https://doi.org/10.1017/S0033822200045288>.
- Walker, M., Head, M.J., Lowe, J., Berkelhammer, M., Björck, S., Cheng, H., Cwynar, L.C., Fisher, D., Gkinis, V., Long, A., Newnham, R., Rasmussen, S.O., Weiss, H., 2019. Subdividing the Holocene Series/Epoch: formalization of stages/ages and subseries/subepochs, and designation of GSSPs and auxiliary stratotypes. *J. Quat. Sci.* 34, 173–186. <https://doi.org/10.1002/jqs.3097>.
- Walker, M.J.C., Gibbard, P.L., Berkelhammer, M., Björck, S., Cwynar, L.C., Fisher, D.A., Long, A.J., Lowe, J.J., Newnham, R.M., Rasmussen, S.O., Weiss, H., 2014. Formal Subdivision of the Holocene series/Epoch. In: Rocha, R., Pais, J., Kullberg, J.C., Finney, S. (Eds.), *STRATI 2013*. Springer Geology. Springer International Publishing, Cham, pp. 983–987. [https://doi.org/10.1007/978-3-319-04364-7\\_186](https://doi.org/10.1007/978-3-319-04364-7_186).
- Waller, M., 1994. *The Fenland Project, Number 9: Flandrian Environmental Change in Fenland, East Anglian Archaeology*. Cambridgeshire Archaeological Committee, Cambridge.
- Waller, M., Early, R., 2015. Vegetation dynamics from a coastal peatland: insights from combined plant macrofossil and pollen data. *J. Quat. Sci.* 30, 779–789.
- Waller, M., Kirby, J., 2021. Coastal peat-beds and peatlands of the southern North Sea: their past, present and future. *Biol. Rev.* 96, 408–432. <https://doi.org/10.1111/bvr.12662>.
- Weninger, B., Schulting, R., Bradtmöller, M., Clare, L., Collard, M., Edinborough, K., Hilpert, J., Jöris, O., Niekus, M., Rohling, E.J., Wagner, B., 2008. The catastrophic final flooding of Doggerland by the Storegga Slide tsunami. *Documenta Praehistorica* 35, 1–24. <https://doi.org/10.4312/dp.35.1>.
- West, R.G., 1993. On the history of the late Devensian lake Sparks in southern Fenland, Cambridgeshire, England. *J. Quat. Sci.* 8, 217–234. <https://doi.org/10.1002/jqs.3390080304>.
- Wheeler, A.J., 1992. Vegetational succession, acidification and allogenic events as recorded in Flandrian peat deposits from an isolated Fenland embayment. *New Phytol.* 122, 745–756. <https://doi.org/10.1111/j.1469-8137.1992.tb00103.x>.
- Wigley, T.M.L., Briffa, K.R., Jones, P.D., 1984. On the average value of correlated time series, with applications in Dendroclimatology and hydrometeorology. *J. Appl.*

- Meteorol. Climatol. 23, 201–213. [https://doi.org/10.1175/1520-0450\(1984\)023<0201:OTAVOC>2.0.CO;2](https://doi.org/10.1175/1520-0450(1984)023<0201:OTAVOC>2.0.CO;2).
- Yang, B., Qin, C., Bräuning, A., Osborn, T.J., Trouet, V., Ljungqvist, F.C., Esper, J., Schneider, L., Griesinger, J., Büntgen, U., Rossi, S., Dong, G., Yan, M., Ning, L., Wang, J., Wang, X., Wang, S., Luterbacher, J., Cook, E.R., Stenseth, N.Chr., 2021. Long-term decrease in Asian monsoon rainfall and abrupt climate change events over the past 6,700 years. Proc. Natl. Acad. Sci. USA 118, e2102007118. <https://doi.org/10.1073/pnas.2102007118>.
- Yang, B., Qin, C., Wang, J., He, M., Melvin, T.M., Osborn, T.J., Briffa, K.R., 2014. A 3,500-year tree-ring record of annual precipitation on the northeastern Tibetan Plateau. Proc. Natl. Acad. Sci. USA 111, 2903–2908. <https://doi.org/10.1073/pnas.1319238111>.